Int. J. Solids Structures Vol. 24, No. 9, pp. 893–913, 1988
Printed in Great Britain.

0020–7683/88 $3.00+ .00

BEHAVIOR OF BRACED AND UNBRACED SEMI-RIGID FRAMES

ERIC M. LUI
Department of Civil Engineering, Syracuse University, Syracuse, NY 13244-1190, U.S.A.

and

WAI-FAH CHEN
School of Civil Engineering, Purdue University, West Lafayette, IN 47907, U.S.A.

(*Received* 16 *November* 1987; *in revised form* 24 *March* 1988)

Abstract—The state-of-the-art limit states specification for structural steel buildings explicitly acknowledges the semi-rigid nature of most connections by allowing for the construction of semi-rigid frames under its Type PR (Partially Restrained) Construction provision. The construction of semi-rigid frames differs from that of rigid frames in that connection behavior must be taken into consideration in the analysis and design process. This paper attempts to shed light on the subject by outlining a methodology for semi-rigid frame analysis. Analytical studies of both braced and unbraced semi-rigid frames are presented. It is found that the use of bracings not only increases the strength and stiffness of semi-rigid frames, but it drastically reduces the sensitivity of the frames to differences in connection behavior. It is further demonstrated that for design application the assumption of linear connection behavior is quite adequate for braced semi-rigid frames.

NOTATION

A	cross-sectional area
b_1, b_2	bowing coefficients
C_j	curve-fitting constants
$\mathbf{d}_c$	element corotational displacement vector
$\mathbf{d}_g$	element global displacement vector
$\mathbf{D}_s$	structure displacement vector
E	modulus of elasticity
I	moment of inertia
k^2	P/EI
$\mathbf{k}$	element stiffness matrix
k_{ij}	elements of the stiffness matrix
$\mathbf{K}_s$	structure stiffness matrix
L	length
M	moment
M_0	initial connection moment
P	axial force
P_{cr}	critical load
P_y	yield load
$\mathbf{r}$	element load vector
R_k	connection stiffness
$\bar{R}_k$	non-dimensional connection stiffness, LR_k/EI
R_{ki}	initial connection stiffness
R_{kf}	strain-hardening connection stiffness
$\mathbf{R}_s$	structure load vector
s_1, s_2	stability functions
$\mathbf{T}_{cg}$	corotational–global transformation matrix
$\mathbf{T}_i$	initial stress transformation matrix
u	net longitudinal displacement
u_a	longitudinal displacement due to axial effect
u_c	longitudinal displacement due to curvature effect
α	connection model scaling factor
θ	rotation
θ_r	relative rotation
λ_c	slenderness parameter, $(KL\sqrt{(F_y/E)})/r\pi$
ρ	PL^2/π^2EI.

INTRODUCTION

The advent of computers coupled with an increased understanding of structural behavior has advanced design philosophy and design practice into a new era. In the U.S.A., design philosophy for steel structures has emerged from an allowable stress concept and advanced through the plastic design concept into the current stage of the limit states concept. In a limit states approach to design, it is essential to consider all structural components which may affect the limit states behavior of the structure. It has been known for decades that connection flexibility has a definitive influence on structural response. Nevertheless, the incorporation of connection behavior into the analysis and design process is seldom undertaken by designers. This is attributed to the fact that because of the complex geometries of the connection it is rather difficult to assess the behavior of the various types of connections accurately. In addition, most commonly used connections exhibit non-linear behavior. As a result, non-linear structural analysis techniques are often entailed if a semi-rigid procedure is employed.

The state-of-the-art limit states design code for steel building structures currently in use in the U.S.A. is contained in the so-called Load and Resistance Factor Design (LRFD) Specification (1986). In this specification, two types of construction are designated in its provision. Type FR (Fully Restrained) Construction in which the connections are assumed to be rigid; and Type PR (Partially Restrained) Construction in which the connections are assumed to possess a predictable amount of rotational stiffness.

Type FR Construction is analogous to Type 1 (Rigid Framing) in the Allowable Stress Design (ASD) Specification (1978) and Type PR Construction is analogous to Type 3 (Semi-rigid Framing) Construction in the ASD Specification. The ASD Type 2 (Simple Framing) Construction becomes a special case of the LRFD Type PR Construction.

The LRFD provision for Type PR Construction has paved the way for a more realistic and logical design of steel frameworks. Taking into consideration connection flexibility in the analysis and design process represents an important step towards the manifestation of the limit states concept. Although studies on the behavior of flexibly-jointed frames are available in the literature (Gerstle, 1985; Stelmack *et al.*, 1986; Nethercot *et al.*, 1986; Davison *et al.*, 1986; Goto and Chen, 1987; Chen and Zhou, 1987), all these studies are concerned with the assessment of the behavior of bare frames. In the present study, the stability and limit states behavior of semi-rigid frames with bracings will be presented. It was found that the introduction of bracings has a significant influence on frame behavior. It is therefore the intent of this paper to present a methodology for the non-linear large displacement analysis of semi-rigid braced and unbraced frames. A stability study of both braced and unbraced semi-rigid frames will then follow. In addition, the load deflection behavior of these frames will be discussed.

METHOD OF ANALYSIS

An updated Lagrangian approach was employed in the present study in which a moving corotational coordinate attached to the element was related to a fixed global coordinate at each cycle of calculation. Since the problem is intrinsically nonlinear due to the non-linear behavior of the connections as well as the geometrical nonlinearity of the frame, solution is obtained by an iterative procedure and linearization of the problem at each cycle of calculation is effected by the tangent stiffness approach.

MODELING OF CONNECTION ELEMENT

The connection element used in the present study is a two degrees-of-freedom non-linear spring element shown in Fig. 1. The incremental element force–displacement relationship has the form

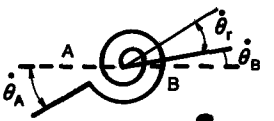

Fig. 1. Schematic representation of a connection.

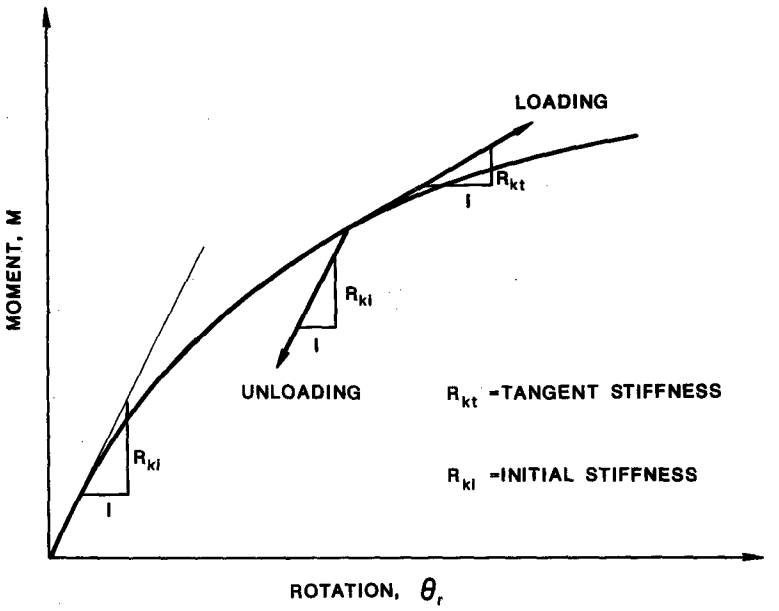

Fig. 2. Loading–unloading behavior of connections.

$$\begin{pmatrix} \dot{M}_A \\ \dot{M}_B \end{pmatrix} = \begin{bmatrix} R_k & -R_k \\ -R_k & R_k \end{bmatrix} \begin{pmatrix} \dot{\theta}_A \\ \dot{\theta}_B \end{pmatrix} \tag{1}$$

where $\dot{M}_A$, $\dot{M}_B$, $\dot{\theta}_A$, $\dot{\theta}_B$ are the incremental moment and rotation at the Ath and Bth ends of the connection, respectively. R_k is the instantaneous stiffness of the connection. It is represented by the slope of the moment–rotation ($M-\theta_r$) curve of the connection. If the moment–rotation behavior of the connection is represented by a function of the form

$$M = \sum_{j=1}^{n} C_j[1-\exp(-|\theta_r|/2j\alpha)] + R_{kf}|\theta_r| + M_0 \tag{2}$$

then (refer to Fig. 2) the expressions for R_k can be written as

$$R_{kt} = \mathrm{d}M/\mathrm{d}\theta_r|_{|\theta_r|=|\theta_r|} = \sum_{j=1}^{n} \frac{C_j}{2j\alpha}[\exp(-|\theta_r|/2j\alpha)] + R_{kf} \tag{3a}$$

if the connection loads, and

$$R_{ki} = \mathrm{d}M/\mathrm{d}\theta_r|_{|\theta_r|=0} = \sum_{j=1}^{n} \frac{C_j}{2j\alpha} + R_{kf} \tag{3b}$$

if the connection unloads.

In the above equations M is the moment in the connection, $|\theta_r|$ the absolute value of the rotational deformation of the connection, R_{kf} the strain-hardening stiffness of the connection, M_0 the initial moment, α a scaling factor, and C_j curve-fitting constants.

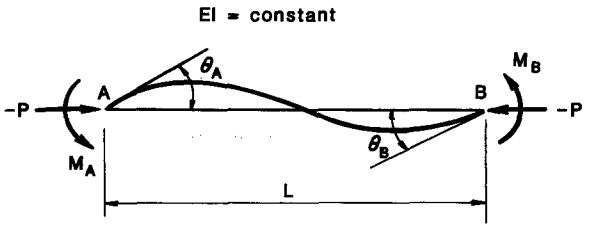

Fig. 3. Beam–column element.

MODELING OF BEAM–COLUMN ELEMENT

Consider a prismatic beam–column element of length L and moment of inertia I with modulus of elasticity E as shown in Fig. 3, the moment–rotation relationship of this element has the familiar form

$$\begin{pmatrix} M_A \\ M_B \end{pmatrix} = \frac{EI}{L}\begin{bmatrix} s_1 & s_2 \\ s_2 & s_1 \end{bmatrix}\begin{pmatrix} \theta_A \\ \theta_B \end{pmatrix} \tag{4}$$

where M_A, M_B, θ_A, θ_B are the bending moments and the corresponding joint rotations at the Ath and Bth ends of the element, respectively. s_1 and s_2 are the well-known stability functions which account for the effect of the axial force on the bending stiffness of the member. For the present study, these stability functions are expressed as

$$s_1 = 4+2\pi^2\rho/15\rho-[(0.010\rho+0.543)/(4+\rho)+(0.004\rho+0.285)/(8.183+\rho)]\rho^2 \tag{5a}$$

$$s_2 = 2-\pi^2\rho/30+[(0.010\rho+0.543)/(4+\rho)-(0.004\rho+0.285)/(8.183+\rho)]\rho^2 \tag{5b}$$

where

$$\rho = PL^2/\pi^2EI.$$

Detailed derivations of the above expressions have been given previously (Lui, 1985). Nevertheless, it should be pointed out that eqns (5a) and (5b) apply regardless of whether the axial form is tensile (positive P) or compressive (negative P). Consequently, the use of these expressions in a numerical analysis represents an advantage over the conventional expressions in which slightly different forms exist for the tensile and compressive axial force cases.

If the effect of bending curvature is taken into account, the axial force–displacement relationship for the element can be written as

$$P = \frac{EA}{L}u_a = \frac{EA}{L}(u+u_c) \tag{6}$$

where u_a is the longitudinal displacement due to the axial effect only, u the net longitudinal displacement, u_c the longitudinal displacement due to the curvature effect only, which can be expressed in terms of θ_A and θ_B

$$u_c = [b_1(\theta_A+\theta_B)^2+b_2(\theta_A-\theta_B)^2]L \tag{7}$$

where

$$b_1 = \frac{(s_1+s_2)(s_2-2)}{8\pi^2\rho} \tag{8a}$$

$$b_2 = \frac{s_2}{8(s_1+s_2)}. \tag{8b}$$

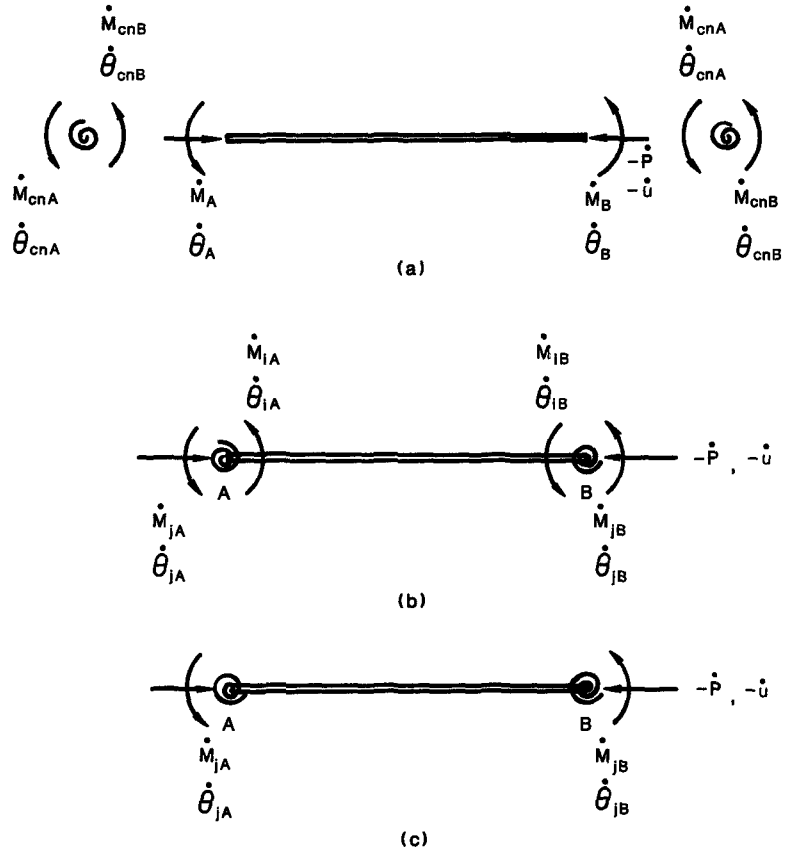

Fig. 4. Modified beam–column element.

Equations (4) and (6) can be combined and expressed in incremental form by taking derivatives of the expressions for M_A, M_B and P with respect to a time-like variable. The resulting equations, after omitting higher order terms involving squares and products of θ_A and θ_B, have the form

$$\begin{pmatrix} \dot{M}_A \\ \dot{M}_B \\ \dot{P} \end{pmatrix} = \frac{EI}{L} \begin{bmatrix} k_{c11} & k_{c12} & k_{c13} \\ & k_{c22} & k_{c23} \\ \text{sym.} & & k_{c33} \end{bmatrix} \begin{pmatrix} \dot{\theta}_A \\ \dot{\theta}_B \\ \dot{u} \end{pmatrix} \tag{9}$$

where

$$k_{c11} = s_1$$

$$k_{c12} = s_2$$

$$k_{c13} = 2AL[(b_1+b_2)\theta_A+(b_1-b_2)\theta_B]/I$$

$$k_{c22} = k_{c11}$$

$$k_{c23} = 2AL[(b_1-b_2)\theta_A+(b_1+b_2)\theta_B]/I$$

$$k_{c33} = A/I.$$

Equation (9) is the incremental basic stiffness relationship of a beam–column element the ends of which are rigidly connected to other elements. If connections are present at the ends, modification of this equation is necessary. This modification is shown schematically in Fig. 4. An intermediate element is first formed by combining the connection elements

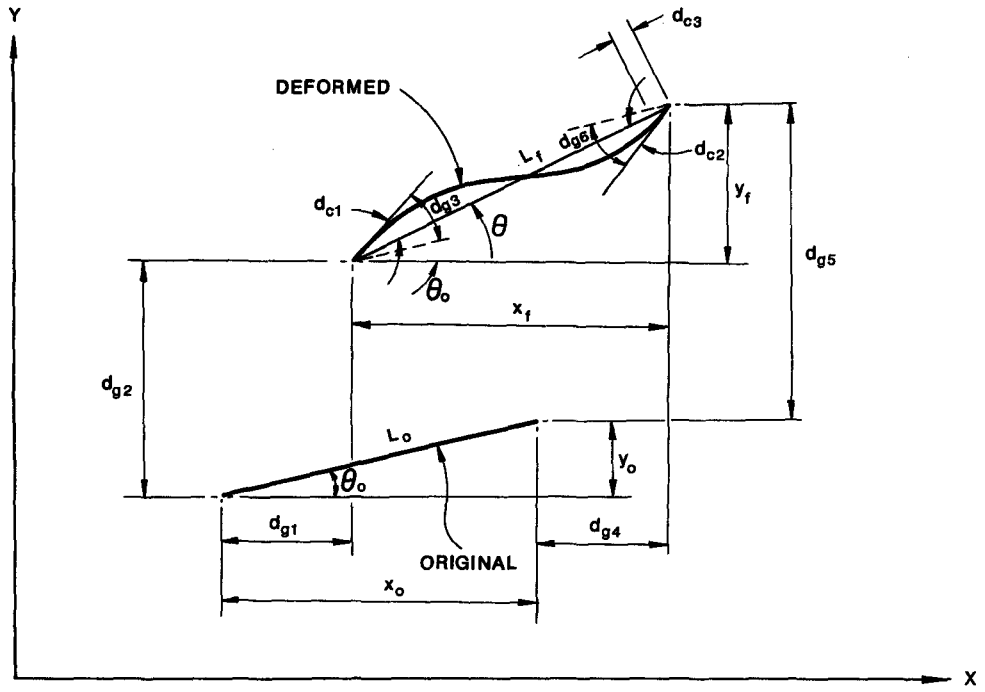

Fig. 5. Kinematic relationships between basic and global displacements of a beam–column element.

with the beam–column element (Fig. 4(b)). The internal degrees of freedom of this element are then condensed out of the stiffness relationship using a standard static condensation technique. The resulting element is shown in Fig. 4(c). The incremental force–displacement relationship of this element is expressed by

$$\begin{pmatrix} \dot{M}_{jA} \\ \dot{M}_{jB} \\ \dot{P} \end{pmatrix} = \frac{EI}{L} \begin{bmatrix} s_{c11} & s_{c12} & s_{c13} \\ & s_{c22} & s_{c23} \\ \text{sym.} & & s_{c33} \end{bmatrix} \begin{pmatrix} \dot{\theta}_{jA} \\ \dot{\theta}_{jB} \\ \dot{u} \end{pmatrix} \tag{10}$$

where

$$\begin{aligned}
s_{c11} &= \bar{R}_{kA} - \bar{R}_{kA}^2(\bar{R}_{kB} + k_{c22})/\bar{R}_k^* \\
s_{c12} &= \bar{R}_{kA}\bar{R}_{kB}k_{c12}/\bar{R}_k^* \\
s_{c13} &= [\bar{R}_{kA}k_{c13}(\bar{R}_{kB} + k_{c22}) - \bar{R}_{kA}k_{c12}k_{c23}]/\bar{R}_k^* \\
s_{c22} &= \bar{R}_{kB} - \bar{R}_{kB}^2(R_{kA} + k_{c11})/\bar{R}_k^* \\
s_{c23} &= [\bar{R}_{kB}k_{c23}(\bar{R}_{kA} + k_{c11}) - \bar{R}_{kB}k_{c12}k_{c13}]/\bar{R}_k^* \\
s_{c33} &= k_{c33} - [k_{c13}^2(\bar{R}_{kB} + k_{c22}) + k_{c23}^2(\bar{R}_{kA} + k_{c11}) - 2k_{c12}k_{c23}k_{c13}]/\bar{R}_k^* \\
\bar{R}_k^* &= (\bar{R}_{kA} + k_{c11})(\bar{R}_{kB} + k_{c22}) - k_{c12}^2.
\end{aligned}$$

Symbolically, eqn (10) can be written as

$$\dot{\mathbf{r}}_c = \mathbf{k}_c\dot{\mathbf{d}}_c. \tag{11}$$

It should be pointed out that the basic tangent stiffness relationship expressed in the above equation does not take into account the rigid body motion of the member. For a plane frame member, three additional degrees of freedom are required to completely describe the displaced configuration of the member. If we define $d_{g1}, d_{g2}, \ldots, d_{g6}$ as the global translational and rotational degrees of freedom of a beam–column member (Fig. 5), it can easily be shown that the basic displacements are related to the global displacements by

$$d_{c1} = \theta_{jA} = \theta_0 + d_{g3} - \tan^{-1}\frac{y_0 + d_{g5} - d_{g2}}{x_0 + d_{g4} - d_{g1}} \tag{12a}$$

$$d_{c2} = \theta_{jB} = \theta_0 + d_{g6} - \tan^{-1}\frac{y_0 + d_{g5} - d_{g2}}{x_0 + d_{g4} - d_{g1}} \tag{12b}$$

$$d_{c3} = u = \sqrt{((x_0 + d_{g4} - d_{g1})^2 + (y_0 + d_{g5} - d_{g2})^2)} - L. \tag{12c}$$

Upon differentiation of eqns (12a)–(12c) with respect to each global degree of freedom, the incremental kinematic relationship relating to two sets of displacement vectors can be written as

$$\dot{\mathbf{d}}_c = \mathbf{T}_{cg}\dot{\mathbf{d}}_g \tag{13}$$

where

$$\dot{\mathbf{d}}_c = [\dot{\theta}_{jA} \quad \dot{\theta}_{jB} \quad \dot{u}]^T$$

$$\dot{\mathbf{d}}_g = [\dot{\mathbf{d}}_{g1} \quad \dot{\mathbf{d}}_{g2} \quad \dot{\mathbf{d}}_{g3} \quad \dot{\mathbf{d}}_{g4} \quad \dot{\mathbf{d}}_{g5} \quad \dot{\mathbf{d}}_{g6}]^T$$

$$\mathbf{T}_{cg} = \begin{bmatrix} -s/L_f & c/L_f & 1 & s/L_f & -c/L_f & 0 \\ -s/L_f & c/L_f & 0 & s/L_f & -c/L_f & 1 \\ -c & -s & 0 & c & s & 0 \end{bmatrix} \tag{14}$$

in which $c = \cos\theta$, $s = \sin\theta$, θ and L_f are the inclination and length of the chord of the deformed member, respectively.

By the contragredient law, the forces in the two systems are related by

$$\mathbf{r}_g = \mathbf{T}_{cg}^T\mathbf{r}_c. \tag{15}$$

Taking derivatives on both sides of eqn (15) gives

$$\dot{\mathbf{r}}_g = \mathbf{T}_{cg}^T\dot{\mathbf{r}}_c + \dot{\mathbf{T}}_{cg}^T\mathbf{r}_c. \tag{16}$$

In view of eqns (11) and (13), we have upon substitution

$$\dot{\mathbf{r}}_g = \mathbf{T}_{cg}^T\mathbf{k}_c\mathbf{T}_{cg}\dot{\mathbf{d}}_g + \dot{\mathbf{T}}_{cg}^T\mathbf{r}_c \tag{17}$$

or

$$\dot{\mathbf{r}}_g = (\mathbf{T}_{cg}^T\mathbf{k}_c\mathbf{T}_{cg} + \mathbf{T}_i\mathbf{r}_{ci})\dot{\mathbf{d}}_g = \mathbf{k}_g\dot{\mathbf{d}}_g, \quad i = 1, 2, 3 \tag{18}$$

where

$$\mathbf{T}_1 = \mathbf{T}_2 = \frac{1}{L_f^2}\begin{bmatrix} -2sc & c^2-s^2 & 0 & 2sc & -(c^2-s^2) & 0 \\ & 2cs & 0 & -(c^2-s^2) & -2sc & 0 \\ & & 0 & 0 & 0 & 0 \\ \text{sym.} & & & -2sc & c^2-s^2 & 0 \\ & & & & 2sc & 0 \\ & & & & & 0 \end{bmatrix} \tag{19}$$

$$\mathbf{T}_3 = \frac{1}{L_f}\begin{bmatrix} s^2 & -sc & 0 & -s^2 & sc & 0 \\ & c^2 & 0 & sc & -c^2 & 0 \\ & & 0 & 0 & 0 & 0 \\ \text{sym.} & & & s^2 & -sc & 0 \\ & & & & c^2 & 0 \\ & & & & & 0 \end{bmatrix}. \tag{20}$$

Equation (18) is the desired member tangent stiffness relationship.

EFFECT OF MEMBER INELASTICITY

The present study accounts for member inelasticity by allowing plastic hinges to be formed at the end(s) of the member. The presence of a plastic hinge changes the stiffness relationship of the member. Thus, further modification of $\mathbf{k}_c$ is necessary. This modification has been described in detail (Lui, 1985). The allowance for plastic hinge formation is essential in a limit state analysis of semi-rigid frames.

MODELING OF BRACING ELEMENTS

The tangent stiffness relationship for a bracing element can easily be obtained from the tangent stiffness relationship of a beam–column element by deleting the appropriate rows and columns in eqn (18) that correspond to the rotational degrees of freedom of the element.

Thus, the tangent stiffness relationship for the bracing element is

$$\dot{\mathbf{r}}_g = (\mathbf{T}_{cg}^T \mathbf{k}_c \mathbf{T}_{cg} + \mathbf{T}P)\dot{\mathbf{d}}_g = \mathbf{k}_g \dot{\mathbf{d}}_g \tag{21}$$

where (refer to Fig. 6)

$$\dot{\mathbf{r}}_g = [\dot{r}_{g1} \quad \dot{r}_{g2} \quad \dot{r}_{g3} \quad \dot{r}_{g4}]^T$$

$$\dot{\mathbf{d}}_g = [\dot{\mathbf{d}}_{g1} \quad \dot{\mathbf{d}}_{g2} \quad \dot{\mathbf{d}}_{g3} \quad \dot{\mathbf{d}}_{g4}]^T$$

$$\mathbf{T}_{cg} = [-c \quad -s \quad c \quad s]$$

$$\mathbf{k}_c = EA/L$$

$$\mathbf{T} = \frac{1}{L_f}\begin{bmatrix} s^2 & -sc & -s^2 & sc \\ & c^2 & sc & -c^2 \\ \text{sym.} & & s^2 & -sc \\ & & & c^2 \end{bmatrix}$$

in which $s = \sin\theta$, $c = \cos\theta$, θ is the inclination of the displaced element, and L_f the final length of the displaced element.

COMPUTATION TECHNIQUE

The stiffness method of analysis was used in the present investigation. The structure tangent stiffness matrix $\mathbf{K}_s$ is formed by assembling all the element tangent stiffness matrices. The structure incremental force–displacement relationship has the form

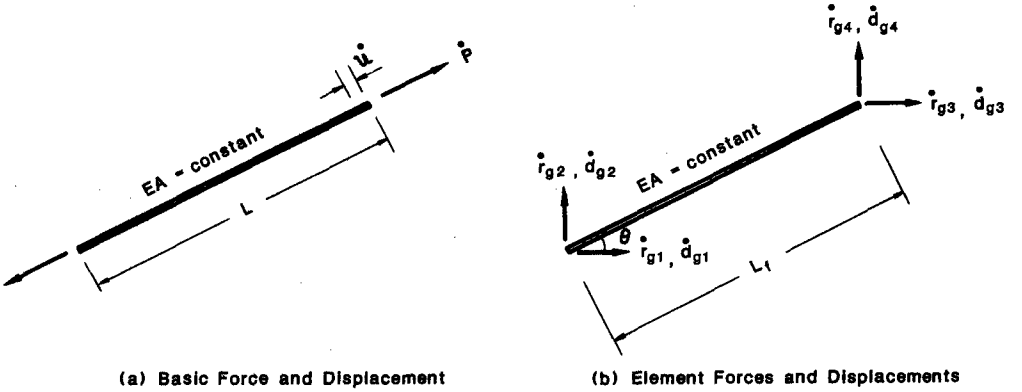

(a) Basic Force and Displacement (b) Element Forces and Displacements

Fig. 6. Bracing element.

$$\dot{\mathbf{R}}_s = \mathbf{K}_s \dot{\mathbf{D}}_s. \tag{22}$$

For a prescribed load increment $\dot{\mathbf{R}}_s$, the structure displacement increment $\dot{\mathbf{D}}_s$ can be solved from eqn (22). This displacement increment is then added to the cumulative structure displacement evaluated at the end of the previous calculation cycle to update the displacement configuration of the structure. However, due to the linearization process, this updated displacement configuration deviates from the "true" displacement configuration of the structure. Consequently, the internal forces which are calculated based on the calculated displacement vector do not balance the external applied forces. The difference between the internal and external force vectors gives an unbalanced force vector which is used as the vector $\dot{\mathbf{R}}_s$ in eqn (22) to get a displacement correction vector $\dot{\mathbf{D}}_s$ in subsequent cycles of calculation. This displacement correction vector is then used to update the structure displacement configuration.

The above process is repeated until the displacement correction vector is sufficiently small to be neglected. The structure tangent stiffness matrix $\mathbf{K}_s$ is updated at every cycle of calculation to accelerate convergence. When convergence is achieved (i.e. when $\dot{\mathbf{D}}_s$ is negligible) at a particular load step, a second load increment is then applied and the whole iterative process is repeated. Thus, by continuing the procedure, the load–displacement response of the frame can be traced.

NUMERICAL STUDIES

A computer program has been written to implement the foregoing formulation for the large displacement elastic–plastic hinge analysis of semi-rigid frames. As mentioned in the preceding section, a load control Newton–Raphson iterative technique was used to trace the load–deflection curve of the frame. In this section, three example problems will be discussed to illustrate the behavior of braced and unbraced semi-rigid frames.

Example 1. *Elastic buckling load of a simple portal semi-rigid frame*

In order to verify the validity of the proposed method and the computer program, the elastic buckling load of a simple portal frame is evaluated using the computer program and checked against its theoretical value. The simple portal frame is shown in Fig. 7(a). The beam is connected to the columns by two connections having a constant connection stiffness of R_k. If E, I and L are constants for all members, the characteristic equation governing the sway buckling behavior of the frame is given by

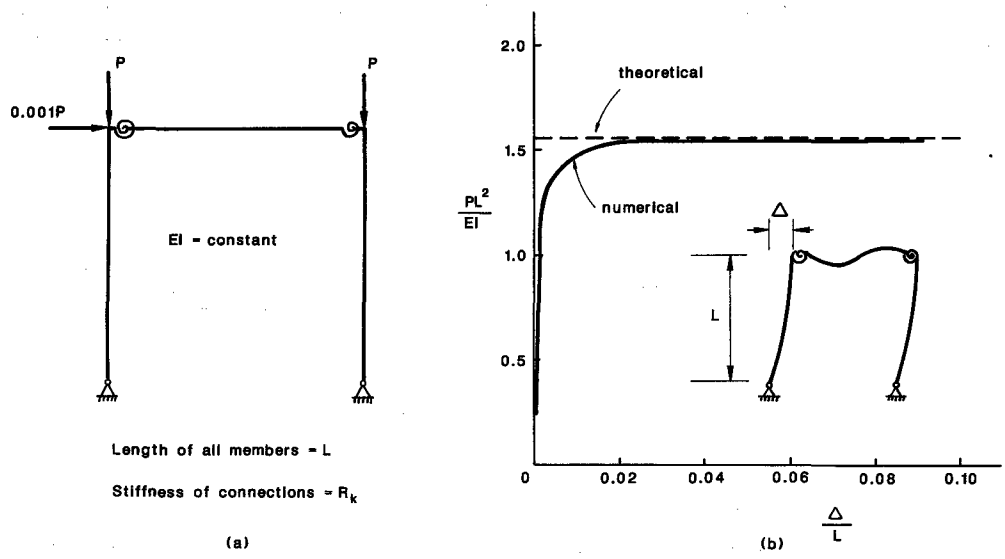

Fig. 7. Elastic buckling load of a semi-rigid simple portal frame.

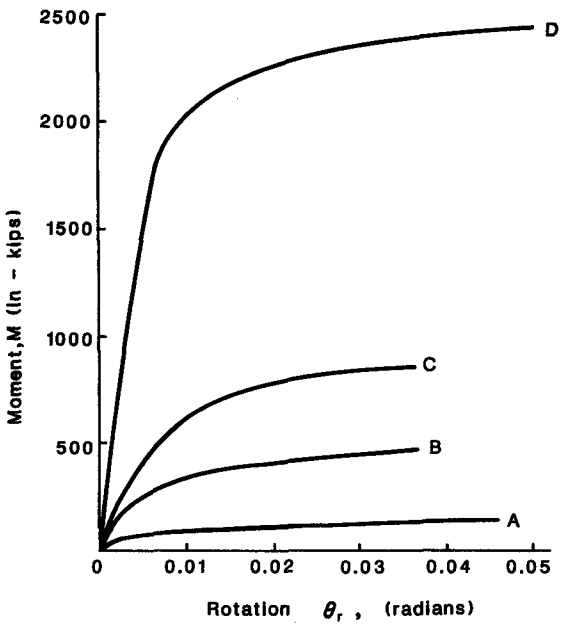

Fig. 8. Connection types used in the study.

$$RS-(R+S)(kL)^2 = 0 \tag{23}$$

where

$$R = (6+12EI/LR_k)/[1+8EI/LR_k+12(EI/LR_k)^2]$$
$$S = s_1 - s_2^2/s_1$$
$$k^2 = P/EI.$$

For the specific case when $EI/LR_k = 0.1$, it can readily be shown that eqn (23) will be satisfied if $kL = 1.25$ from which $P_{cr} = 1.56EI/L^2$. This theoretical value for P_{cr} is plotted in Fig. 7(b) as a horizontal dashed line.

By using the computer program, a numerical value for P_{cr} can be obtained by identifying the peak point of the load–deflection curve. To induce sway, a small horizontal force of $0.001P$ where P is the applied column load was applied to the frame. This lateral force was increased proportionally with the column load P throughout the analysis. Each member of the frame was modeled by two elements. As can be seen from Fig. 7(b) the load–deflection curve generated by the computer approaches asymptotically to the theoretical value for P_{cr}.

Example 2. *Elastic stability limit load of a two-story braced and unbraced semi-rigid frame with different support conditions*

For this example, a more realistic representation of connection behavior is used. The connections are modeled by non-linear curves according to eqn (2). Five types of connections are used in the analyses. They are labeled connections A, B, C, D and rigid in Fig. 8. Connection A is a single web angle connection tested by Richard *et al.* (1982). Connection B is a top and seated angle connection with double web cleats tested by Azizinamini *et al.* (1985). Connection C is a flush end plate connection tested by Ostrander (1970) and connection D is an extended end plate connection tested by Johnson and Walpole (1981). The exponential model parameters for connections are listed in Table 1.

The frame to be analyzed is a two-story frame as shown in Fig. 9. The beams are W 14×48 sections and the columns are W 12×96 sections. Connections are present at every beam–column joint. The beams and columns were selected because their sizes were comparable to those used in the actual testings of the connections. The beams were modeled

Table 1. Connection parameters of the exponential model

	Connection			
	A	B	C	D
M_0	0	0	0	0
R_{kf}	0.47104×10^2	0.43169×10^3	0.96415×10^3	0.41193×10^3
α	0.51167×10^{-3}	0.31425×10^{-3}	0.31783×10^{-3}	0.67083×10^{-3}
C_1	-0.43300×10^2	-0.34515×10^3	-0.25038×10^3	-0.67824×10^3
C_2	0.12139×10^4	0.52345×10^4	0.50736×10^4	0.27084×10^4
C_3	-0.58583×10^4	-0.26762×10^5	-0.30396×10^5	-0.21389×10^5
C_4	0.12971×10^5	0.61920×10^5	0.75338×10^5	0.78563×10^5
C_5	-0.13374×10^5	-0.65114×10^5	-0.82873×10^5	-0.99740×10^5
C_6	0.52224×10^4	0.25506×10^5	0.33927×10^5	0.43042×10^5
R_{ki}	0.48000×10^5	0.95219×10^5	0.11000×10^6	0.30800×10^6

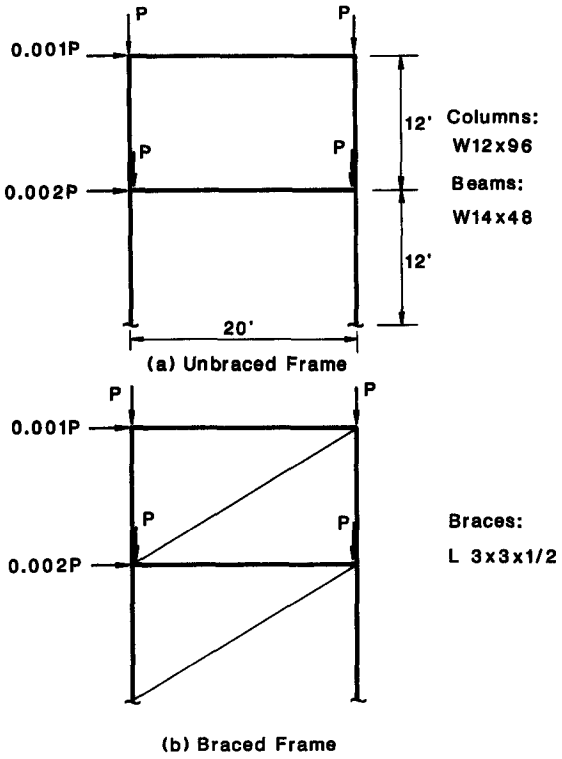

Fig. 9. Two-story frame.

by two elements and the columns by one element in the structure model. As in the first example, small lateral forces are applied to the frame to induce sway. The magnitude of the lateral forces are $0.001P$ for the top story and $0.002P$ for the bottom story. For each connection type, both unbraced and braced cases were analyzed for the frame. For the braced cases, diagonal braces made of angles $L\,3 \times 3 \times \frac{1}{2}$ were used for both stories. In order to investigate the effect of support conditions on frame behavior, all the frames were analyzed by assuming: (1) pinned support case; (2) elastic support case; (3) fixed support case. For the elastic support case, the support is modeled by a linear spring with a spring constant R_{ks} of $0.1(EI/L)_c$ in which subscript c refers to the column.

Figures 10–15 show the load–deflection curves of the frames analyzed. The elastic stability limit loads obtained as the peak points of these curves are summarized in Table 2. Based on this study, several important observations can be made.

(1) The use of bracings greatly increased the stability limit loads of semi-rigid frames. The effect is more pronounced for the more flexible connections. This fact is illustrated in Table 3 in which values for the ratio $(P_{cr})_{\text{with bracings}}/(P_{cr})_{\text{without bracings}}$ for all the different frame cases are shown. It can be seen that regardless of the support conditions, the increase in P_{cr}

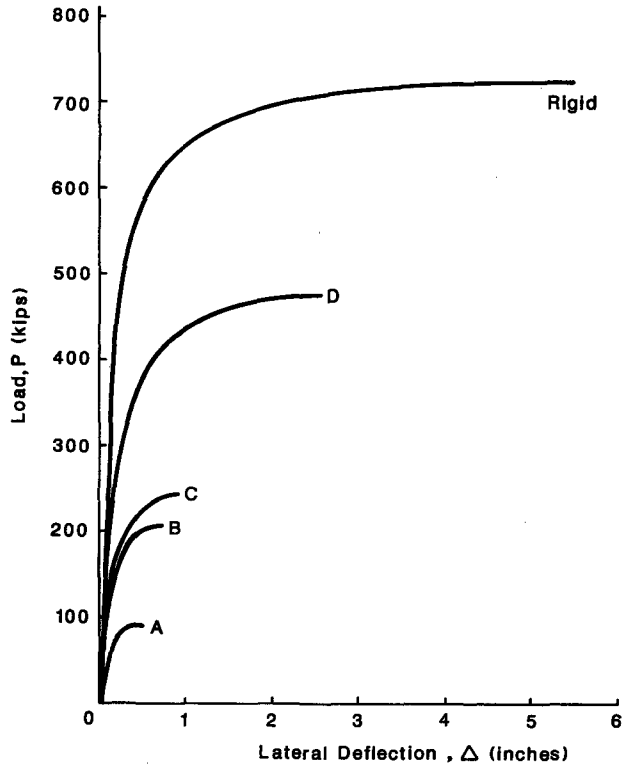

Fig. 10. Elastic load–deflection curves (pinned support, unbraced frame).

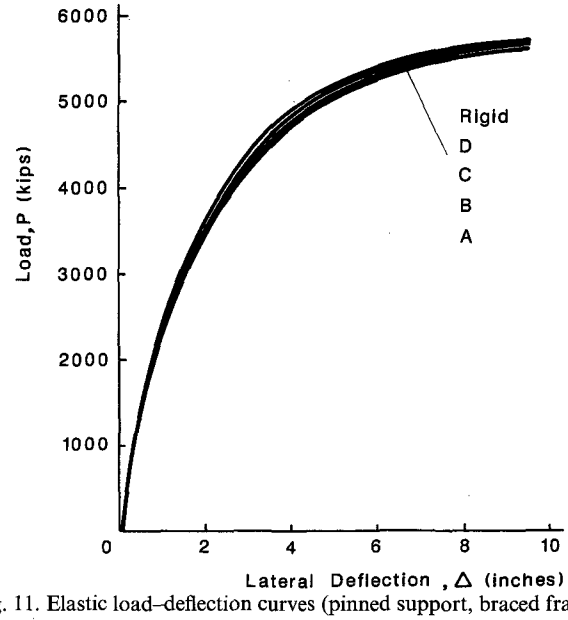

Fig. 11. Elastic load–deflection curves (pinned support, braced frame).

is the most for the most flexible connection indicating that bracings are more effective for the more flexible frame. The increase in P_{cr} is as much as 61.8 times for the pinned support case with connection A whereas the increase is only 3.16 times for the fixed support case with rigid connections. This phenomenon can be explained by the fact that as the rigidity of the connections decreases, the load carrying mechanism of the frame changes from primarily frame action to primarily truss action. Thus, as long as the bracing members remain effective, the frame can always carry the applied load by truss type action.

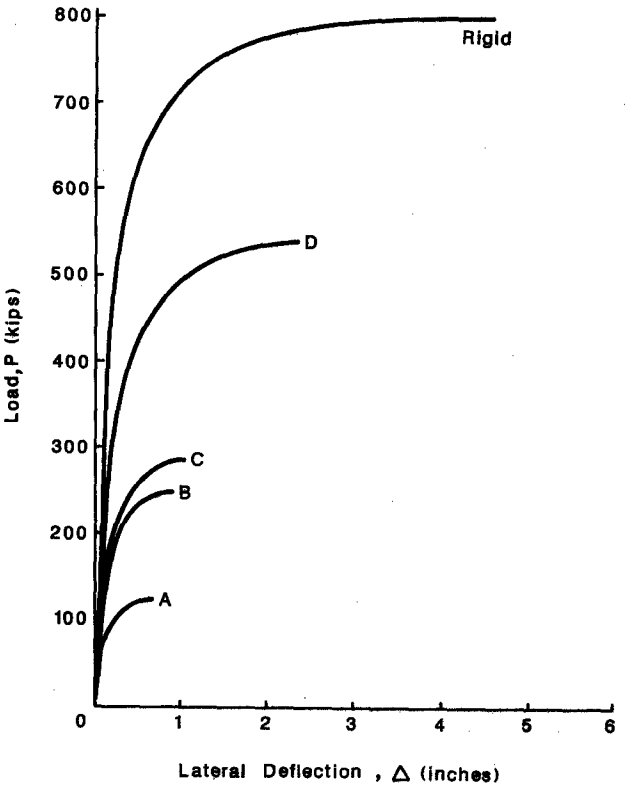

Fig. 12. Elastic load–deflection curves (elastic support, unbraced frame).

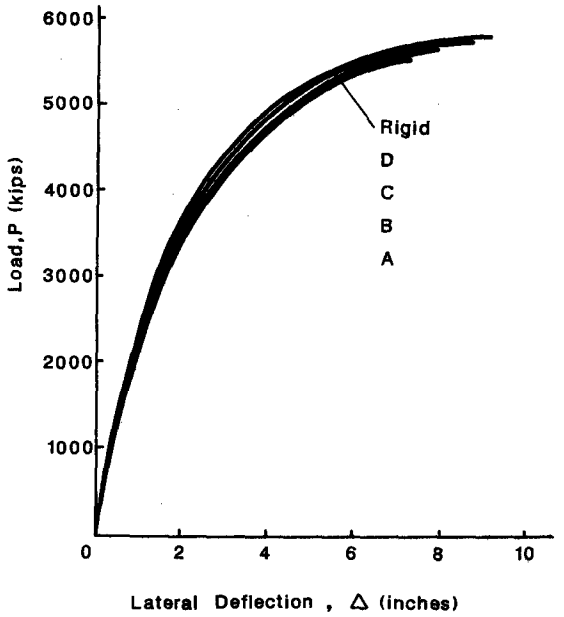

Fig. 13. Elastic load–deflection curves (elastic support, braced frame).

(2) The sensitivity of the frames to difference in connection flexibility is greatly reduced if bracings are provided. It is obvious from Figs 10–15 that the "spread" of the stability limit loads for braced frames are much less than that of the corresponding unbraced frames. This fact is further illustrated in Table 4 in which values of the ratio $(P_{cr})_{\text{flexible connections}}/(P_{cr})_{\text{rigid connections}}$ are shown. For example, for the pinned support case the ratio varies from 0.124 to 1 for the unbraced frames whereas it varies only from 0.986 to 1 for the braced frames. The same conclusion can be made for the elastic and rigid sup-

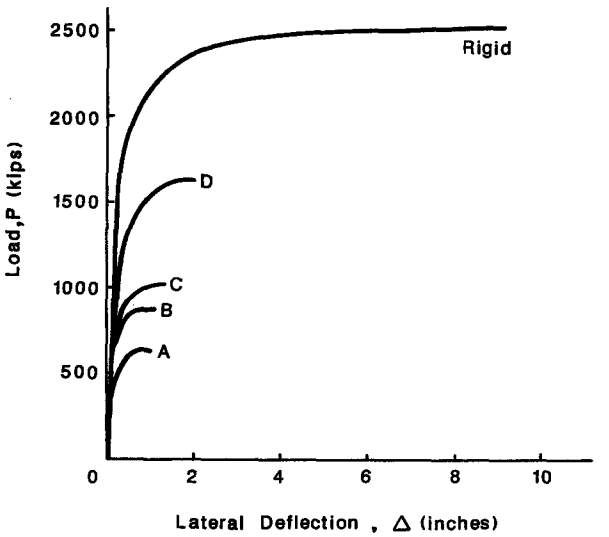

Fig. 14. Elastic load–deflection curves (fixed support, unbraced frame).

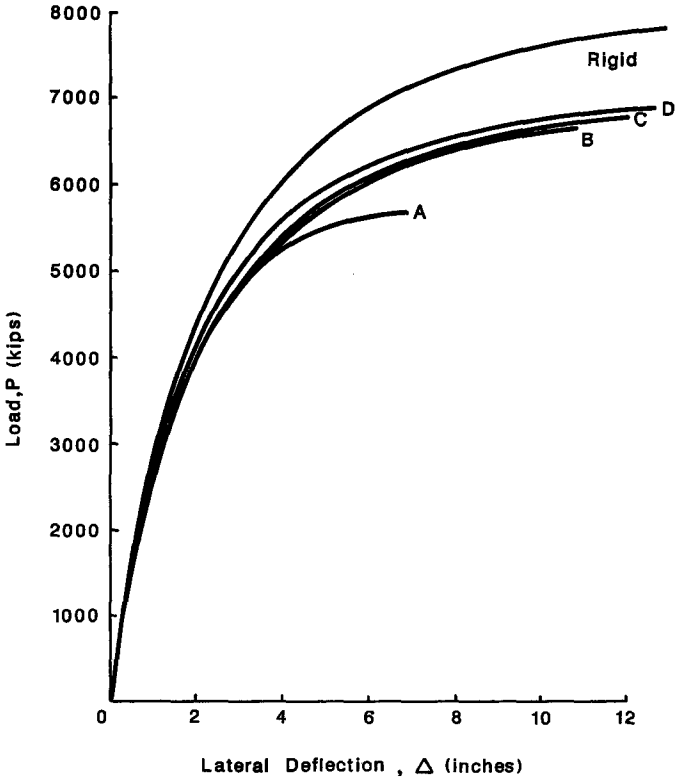

Fig. 15. Elastic load–deflection curves (fixed support, braced frame).

port cases although the reduction in spread is obviously more important for the pinned case.

(3) The effect of support conditions on the stability limit load of semi-rigid frames is less important for braced frames than for unbraced frames. This fact is illustrated in Table 5. If we compare the values for the column under the heading without bracings to that under the heading with bracings for the elastic and fixed support cases, it can readily be seen that the increase in P_{cr} as a result of support fixity is greatly diminished.

The above observations have rather important implications in the stability design of semi-rigid frames. It is common practice to provide bracings to frames to reduce frame

Table 2. Elastic stability limit loads of the two-story frame, kips (kN)

	Pinned support		Elastic support		Fixed support	
	Without bracings	With bracings	Without bracings	With bracings	Without bracings	With bracings
Connection A	90 (400)	5560 (24 700)	125 (556)	5600 (24 900)	630 (2800)	5680 (25 300)
Connection B	205 (912)	5620 (25 000)	250 (1110)	5680 (25 300)	860 (3830)	6680 (29 700)
Connection C	242 (1080)	5620 (25 000)	286 (1270)	5680 (25 300)	1030 (4580)	6850 (30 500)
Connection D	475 (2110)	5630 (25 050)	540 (2400)	5760 (25 600)	1625 (7230)	6940 (30 900)
Rigid connection	725 (3230)	5640 (25 100)	800 (3560)	5800 (25 800)	2530 (11 260)	8000 (35 600)

Table 3. Values of $(P_{cr})_{\text{with bracings}}/(P_{cr})_{\text{without bracings}}$ for the two-story frame

	Pinned support	Elastic support	Fixed support
Connection A	61.8	44.8	9.02
Connection B	27.4	22.7	7.77
Connection C	23.2	19.9	6.65
Connection D	11.9	10.7	4.27
Rigid connection	7.78	7.25	3.16

Table 4. Values of $(P_{cr})_{\text{flexible connection}}/(P_{cr})_{\text{rigid connection}}$ for the two-story frame

	Pinned support		Elastic support		Fixed support	
	Without bracings	With bracings	Without bracings	With bracings	Without bracings	With bracings
Connection A	0.124	0.986	0.156	0.966	0.249	0.710
Connection B	0.283	0.996	0.313	0.979	0.340	0.835
Connection C	0.334	0.996	0.358	0.979	0.407	0.856
Connection D	0.655	0.998	0.675	0.993	0.642	0.868
Rigid connection	1	1	1	1	1	1

Table 5. Values of $(P_{cr})_{\text{elastic support}}/(P_{cr})_{\text{pinned support}}$ and $(P_{cr})_{\text{fixed support}}/(P_{cr})_{\text{pinned support}}$

	$(P_{cr})_{\text{elastic support}}/(P_{cr})_{\text{pinned support}}$		$(P_{cr})_{\text{fixed support}}/(P_{cr})_{\text{pinned support}}$	
	Without bracings	With bracings	Without bracings	With bracings
Connection A	1.39	1.01	7.00	1.02
Connection B	1.22	1.01	4.20	1.19
Connection C	1.18	1.01	4.26	1.22
Connection D	1.14	1.02	3.42	1.23
Rigid connection	1.10	1.03	3.49	1.42

drift as a means to satisfy the serviceability limit state of the design. It has been demonstrated in this study that the provision of bracings not only reduces frame drift but it significantly increases the stability limit load of semi-rigid frames. The increase is more pronounced for the more flexible frames. In fact, the amount of increase is such that it tends to obscure the effect of connection flexibility and support fixity on semi-rigid frames thus allowing the designer to employ a more unified approach to the design of such frames.

Example 3. *Load–deflection behavior of a three-story braced and unbraced frame*

In the preceding example, all members were assumed to behave elastically throughout the entire loading history. Although one may regard this as unrealistic, the use of a simplified material model does have the advantage of allowing us to emphasize the significance of

such parameters as connection flexibility and support fixity on the elastic behavior of semi-rigid frames. The use of elastic analysis is justified for structures within the service load range. In this example, a more realistic structure model will be used, namely, yielding is allowed on the beam and column members in the form of plastic hinges and yielding or buckling is allowed in the bracing members. A plastic hinge is said to have formed on the member when the moment in the member reaches M_{pc} given by

$$M_{pc} = 1.18\left(1 - \frac{P}{P_y}\right)M_p \leqslant M_p \tag{24}$$

where P and P_y are the axial load and yield load of the member, respectively, and M_p is the plastic moment of the member.

Yielding of the bracing member is said to have occurred if

$$P = P_y. \tag{25}$$

Buckling of the bracing member is said tρ have occurred if

$$P = (0.658^{\lambda_c^2})P_y \quad \text{for} \quad \lambda_c \leqslant 1.5 \tag{26a}$$

and

$$P = \left(\frac{0.877}{\lambda_c^2}\right)P_y \quad \text{for} \quad \lambda_c > 1.5. \tag{26b}$$

In eqns (25), (26a) and (26b), P is the axial force in the member and P_y the yield load of the member. $\lambda_c = (KL/r\pi)\sqrt{(F_y/E)}$ in which K is the effective length factor of the members (taken as unity in the present study), r the radius of gyration of the cross-section of the member, and F_y and E are the yield stress and modulus of elasticity of the material, respectively.

The frame to be analyzed is shown in Fig. 16. The columns are made of $W\ 10 \times 88$ sections and the beams are made of $W\ 12 \times 45$ sections. Connections are present in all the beam–column joints. The connections used for this example consist of connections C, D and rigid. Separate analyses were performed for the unbraced (Fig. 16(a)) and braced (Fig. 16(b)) cases. For the braced case, angles made of $L\ 6 \times 6 \times \frac{1}{2}$ sections were used. All the beams were modeled by two elements and all the columns were modeled by one element.

The loadings on the frames are composed of two sequences. In load sequence 1, a load of P was applied at every beam–column joint and a load of $2P$ was applied at midspan of every beam. In addition, lateral loads equal to $0.1P$, $0.2P$ and $0.2P$ were applied at the top, middle and bottom story, respectively (see the left-hand figure of Fig. 16). In load sequence 2, the gravity loads were held constant once they reached 15 kips (66.7 kN) at the beam–column joints and 30 kips (133 kN) at midspan of the beams while the lateral loads continued to increase monotonically until failure (see the right-hand figure of Fig. 16). Failure is said to have occurred when one or more of the following conditions are encountered.

(1) Formation of a collapse mechanism when sufficient plastic hinges have formed.
(2) Failure by frame instability.
(3) Rotational deformation of any connection exceeds 0.05 rad.

The limiting value of 0.05 rad was chosen in conformance with the range of experimental data obtained for the connections used in the study. The results of the analyses for the unbraced and braced cases for the three connections (C, D and rigid) are shown in Figs 17 and 18, respectively. For the unbraced case, the analyses for the frames with connections C and D were terminated when the connections on the leeward side of the frame experienced a rotational deformation in excess of 0.05 rad after plastic hinges were formed at the base. The analysis for the frames with rigid connections was terminated when the frame became

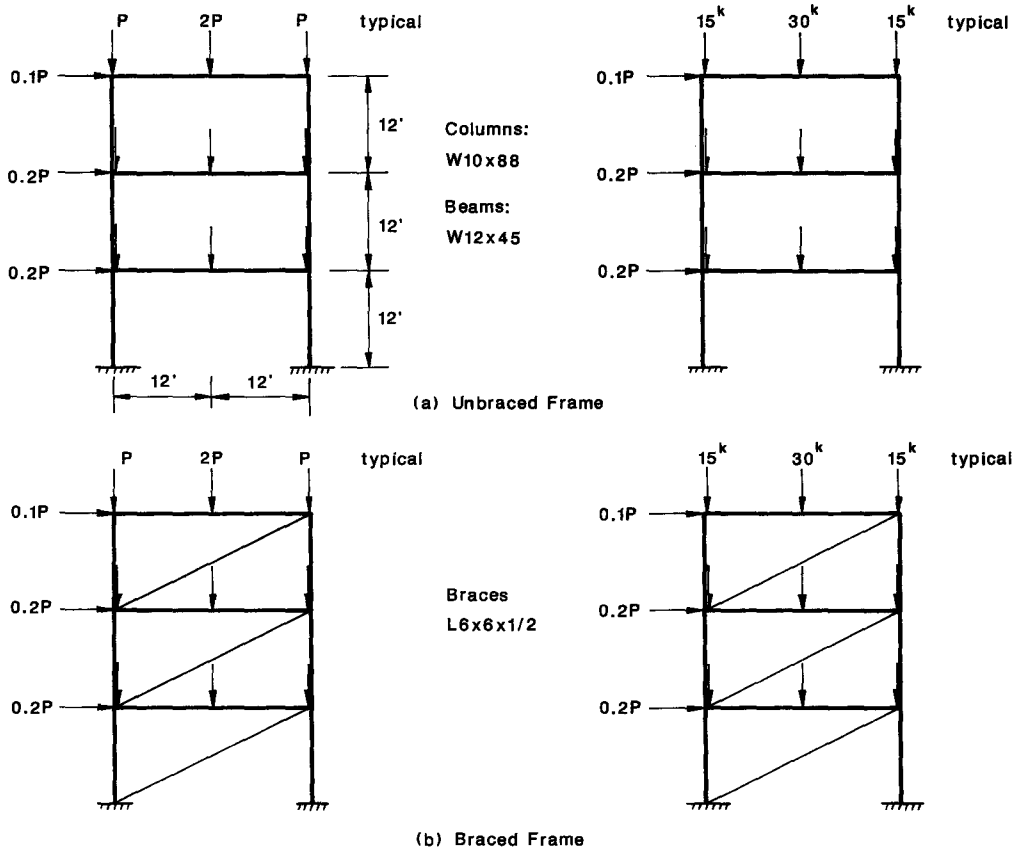

Fig. 16. Three-story frame (load sequences).

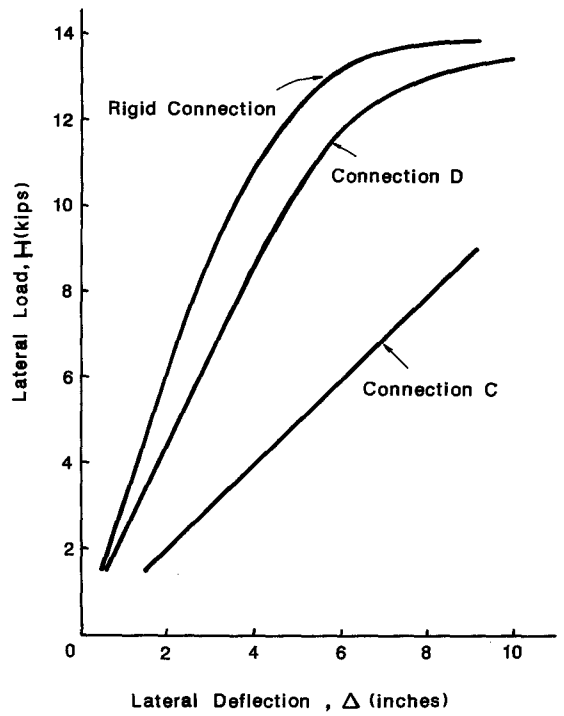

Fig. 17. Load–deflection curves (unbraced frame).

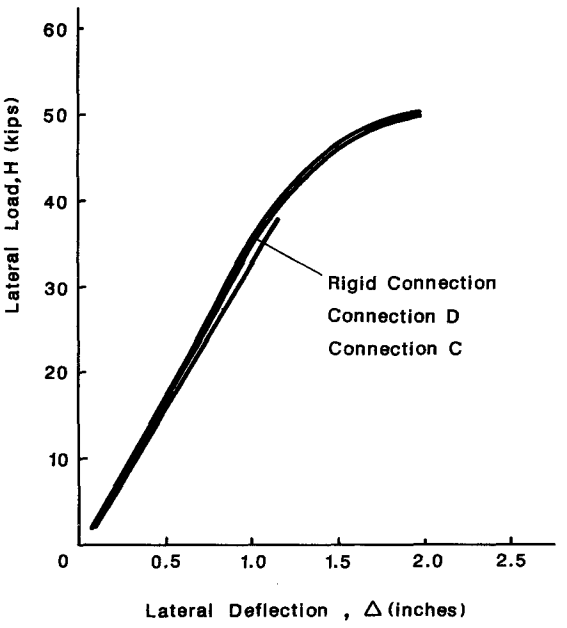

Fig. 18. Load–deflection curves (braced frame).

unstable after the formation of plastic hinges at the base and on the leeward side of beams. For the braced case, the analysis for the frame with connection C was terminated when the rotational deformation of the connection on the leeward side of the first-story beam exceeds 0.05 rad after the formation of a plastic hinge at midspan of the same beam. The analysis for the frames with connection D and rigid connections were terminated when a local mechanism formed in the first-story beam after the diagonal brace of that story had yielded. As can be seen from Fig. 18, the failure loads for the frames with connection D and rigid connections are very close. As for connection C, the failure load is much lower. However, the load–deflection behavior exhibits similar characteristics in the service load range. Careful scrutiny of Figs 17 and 18 indicates that all frames exhibit an almost linear load–deflection behavior for a fairly large range of loadings. This tends to suggest that the effect of connection nonlinearity is not very important in the analysis. To investigate the extent to which connection nonlinearity affects frame behavior, the analyses were repeated for the flexibly connected frames using the assumption of linear connections. The stiffness used for connections C and D were 1.10×10^{10} in. kip rad^{-1} (1.24×10^{9} kN m rad^{-1}) and 3.08×10^{10} in. kip rad^{-1} (3.48×10^{9} kN m rad^{-1}), respectively. The results of these analyses are shown in Figs 19 and 20 for the unbraced and braced cases, respectively.

For the unbraced case, it can be seen from Fig. 19 that although the use of linear connection for the analysis is quite acceptable for the relatively stiff connection D, it is not acceptable for the more flexible connection C. This fact is further illustrated in Tables 6 and 7 in which deflection values at two different load levels are shown for connections C and D, respectively. The two load levels chosen were: (1) the failure load; (2) failure load/

Table 6. Comparison of the effect of connection nonlinearity for the three-story unbraced frame with connection C

	Deflection		
Load kips (kN)	Non-linear connection in. (mm)	Linear connection in. (mm)	Percentage error (%)
6.98 (31.0)	7.00 (178)	4.37 (111)	−37.6
9.07 (40.3)	9.09 (231)	5.45 (138)	−40.0

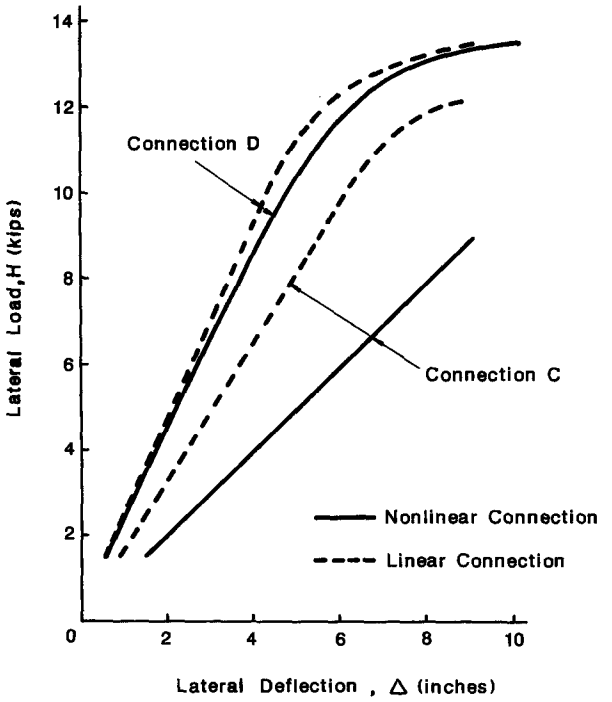

Fig. 19. Comparison of load–deflection behavior of an unbraced frame using linear and non-linear connections.

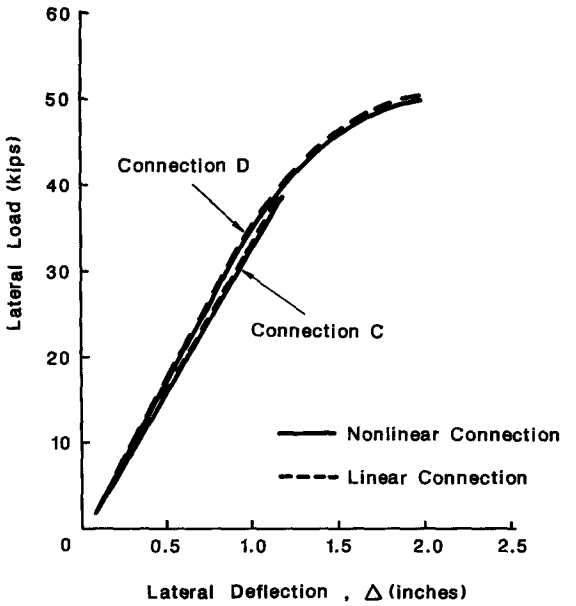

Fig. 20. Comparison of load–deflection behavior of a braced frame using linear and non-linear connections.

1.3. The factor 1.3 is selected because it corresponds to the load factor recommended in Part 2 of the AISC specification (1978). The error introduced by using the assumption of linear connection in the analysis is in the neighborhood of 40% for connection C but it is only around 10% for connection D.

As for the braced case, examination of Fig. 20 shows that the use of the linear connection is acceptable regardless of the flexibility of the connection. The errors introduced are rather insignificant from a practical standpoint (see Tables 8 and 9). This result further

Table 7. Comparison of the effect of connection nonlinearity for the three-story unbraced frame with connection D

Load kips (kN)	Deflection: Non-linear connection in. (mm)	Deflection: Linear connection in. (mm)	Percentage error (%)
10.4 (46.3)	5.09 (129)	4.52 (115)	−11.2
13.5 (60.0)	10.2 (259)	9.2 (234)	−9.8

Table 8. Comparison of the effect of connection nonlinearity for the three-story braced frame with connection C

Load kips (kN)	Deflection: Non-linear connection in. (mm)	Deflection: Linear connection in. (mm)	Percentage error (%)
29.2 (130)	0.907 (23.0)	0.905 (23.0)	−2.21
37.9 (169)	1.15 (29.2)	1.12 (28.4)	−2.61

Table 9. Comparison of the effect of connection nonlinearity for the three-story braced frame with connection D

Load kips (kN)	Deflection: Non-linear connection in. (mm)	Deflection: Linear connection in. (mm)	Percentage error (%)
38.3 (170)	1.13 (28.7)	1.11 (28.2)	−1.77
49.8 (222)	1.88 (47.8)	1.85 (47.0)	−1.60

demonstrates the beneficial effect of providing bracings to semi-rigid frames. By using bracings, the assumption of linear connection behavior in the analysis is more justifiable.

SUMMARY AND CONCLUSIONS

A methodology for the large-displacement elastic and elastic–plastic hinge analysis of semi-rigid frames using the tangent stiffness approach was presented. Analytical studies of braced and unbraced semi-rigid frames have demonstrated that the provision of bracings not only increase the stiffness and strength of semi-rigid fames, but it tends to undermine the effect of connection flexibility in evaluating the elastic stability limit load and the effect of connection nonlinearity on assessing the load–deflection behavior of such frames. Since drift is often a problem for flexibly-connected frames, the use of a lateral load resistant system such as bracings is often indispensable. In view of the present findings, additional benefits from the use of bracings other than drift control can be derived.

REFERENCES

Azizinamini, A., Bradburn, J. H. and Radziminiski, J. B. (1985). Static and cyclic behavior of semi-rigid steel beam–column connections. Technical Report, Department of Civil Engineering, University of South Carolina, Columbia, South Carolina.

Chen, W. F. and Zhou, S. P. (1987). Inelastic analysis of steel braced frames with flexible joints. *Int. J. Solids Structures* **23**, 631–649.

Davison, J. B., Kirby, P. A. and Nethercot, D. A. (1986). Column behavior in PR construction—experimental behavior. ASCE Structures Congress '86, Preprint No. 66-1, New Orleans, Louisiana.

Gerstle, K. H. (1985). Flexibly connected steel frames. In *Steel Framed Structures—Stability and Strength* (Edited by R. Narayanan), Chap. 7, pp. 205–239. Elsevier Applied Science.

Goto, Y. and Chen, W. F. (1987). On the computer-based design analysis for the flexibly jointed frames (Special Issue on Joint Flexibility in Steel Frames). *J. Construct. Steel Res.* **8,** 203–232.

Johnson, N. D. and Walpole, W. R. (1981). Bolted end-plate beam-to-column connections under earthquake type loading. Research Report 81-7, Department of Civil Engineering, University of Canterbury, Christchurch, New Zealand.

Load and Resistance Factor Design Specification for Structural Steel Buildings (1986). American Institute of Steel Construction, Chicago, September.

Lui, E. M. (1985). Effects of connection flexibility and panel zone deformation on the behavior of plane steel frames. Ph.D. Dissertation, School of Civil Engineering, Purdue University, West Lafayette, Indiana.

Nethercot, D. A., Kirby, P. A. and Rifai, A. M. (1986). Design of columns in PR construction—analytical studies. ASCE Structures Congress '86, Preprint No. 66-5, New Orleans, Louisiana.

Ostrander, J. R. (1970). An experimental investigation of end-plate connections. Master's Thesis, University of Saskatchewan, Saskatoon, Saskatchewan, Canada.

Richard, R. M., Kreigh, J. D. and Hormby, D. E. (1982). Design of single plate framing connections with A307 bolts. *Engng J. AISC* **19**(4), Fourth Quarter, 209–213.

Specification for the Design, Fabrication and Erection of Structural Steel for Buildings (1978). American Institute of Steel Construction, Chicago, November.

Stelmack, T. W., Marley, M. J. and Gerstle, K. H. (1986). Analysis and tests of flexibly connected steel frames. *J. Struct. Engng ASCE* **112**(7), 1573–1588.